

DOI: 10.1002/cssc.201402357

Methanol Steam Reforming Promoted by Molten Salt-Modified Platinum on Alumina Catalysts

Matthias Kusche,^[a] Friederike Agel,^[a] Nollaig Ní Bhriain,^[a] Andre Kaftan,^[b] Mathias Laurin,^[b] Jörg Libuda,^[b] and Peter Wasserscheid^{*[a]}

We herein describe a straight forward procedure to increase the performance of platinum-on-alumina catalysts in methanol steam reforming by applying an alkali hydroxide coating according to the “solid catalyst with ionic liquid layer” (SCILL) approach. We demonstrate by diffuse reflectance infrared Fourier transform spectroscopy (DRIFTS) and temperature-programmed desorption (TPD) studies that potassium doping plays an important role in the catalyst activation. Moreover, the hygroscopic nature and the basicity of the salt modification contribute to the considerable enhancement in catalytic

performance. During reaction, a partly liquid film of alkali hydroxides/carbonates forms on the catalyst/alumina surface, thus significantly enhancing the availability of water at the catalytically active sites. Too high catalyst pore fillings with salt introduce a considerable mass transfer barrier into the system as indicated by kinetic studies. Thus, the optimum interplay between beneficial catalyst modification and detrimental mass transfer effects had to be identified and was found on the applied platinum-on-alumina catalyst at KOH loadings around 7.5 mass%.

Introduction

Methanol steam reforming is the method of choice to produce hydrogen from methanol in high yields.^[1] Under optimal process conditions, the reaction converts one mol of methanol and water into carbon dioxide and three mol of hydrogen, as shown in Equation (1).




Nowadays, methanol steam reforming is receiving considerable attention in the context of a methanol-based energy storage and release cycle.^[2] Methanol is considered as a promising candidate to store hydrogen produced by electrolysis with electricity from regenerative excess energies (e.g., from wind and solar). In this context, methanol should not be produced via synthesis gas from fossil energy reserves but by hydrogenation of CO₂. The latter may be recovered from the flue gas of power plants or from the exhaust gas of the cement industry.

To complete the storage cycle, hydrogen release from methanol requires attention. For decentralized hydrogen production, highly efficient hydrogen release under mild conditions is desired, for example, to allow heat integration of the endothermic steam reforming step with available low caloric heat streams. Currently, the upper limit for high-temperature proton exchange membrane (PEM) fuel cells is 180 °C.^[3] It would be highly desirable to efficiently operate methanol steam reforming at this temperature level to provide the necessary heat for the endothermic methanol reforming step from the exothermic operation of the fuel cell. Moreover, the product gas should be virtually free of CO to allow its use in a PEM fuel cell. As CO is a known poison to fuel cell catalysts,^[4] high concentrations of CO in the product gas would require costly additional gas processing steps, such as CO adsorption, preferential oxidation (PROX), or methanation. To fulfil these requirements, the development of more effective catalyst systems for methanol steam reforming is of great technical interest.

For MeOH steam reforming two different classes of heterogeneous catalysts dominate research and industrial practice. The commercial Cu/ZnO systems are indeed very active and selective, but they require lengthy activation procedures. For this purpose, the catalyst is typically brought in contact with a diluted stream of hydrogen for several hours. However, such catalyst preformation is inappropriate for most fluctuating, on-demand hydrogen production scenarios. In addition, copper-based catalysts are highly pyrophoric materials in their activated state and require reasonable treatment to avoid deactivation during standby. These facts complicate the practical handling of copper-based catalysts in dynamic on-off cycles. Catalyst formulations based on noble metals are easier to handle

[a] M. Kusche, Dr. F. Agel, Dr. N. Ní Bhriain, Prof. Dr. P. Wasserscheid
Lehrstuhl für Chemische Reaktionstechnik
Friedrich-Alexander-Universität Erlangen-Nürnberg
Egerlandstrasse 3, 91058 Erlangen (Germany)
Fax: (+49) 9131-8527421
E-mail: wasserscheid@crt.cbi.uni-erlangen.de
Homepage: www.crt.cbi.uni-erlangen.de

[b] A. Kaftan, Dr. M. Laurin, Prof. Dr. J. Libuda
Lehrstuhl für Physikalische Chemie II
Friedrich-Alexander-Universität Erlangen-Nürnberg
Egerlandstrasse 3, 91058 Erlangen (Germany)
Fax: (+49) 9131-8528867

 Supporting Information for this article is available on the WWW under <http://dx.doi.org/10.1002/cssc.201402357>.

and often show immediate start up. Here, especially the use of palladium or platinum on different types of support materials has been reported for the methanol steam reforming reaction.^[5]

As dynamic hydrogen production scenarios are the focus of our research, we investigated in this study the optimization of supported platinum catalysts for methanol steam reforming. We expand here on an earlier communication of our group,^[6] which demonstrated that platinum-on-alumina (Pt/Al₂O₃) catalysts exhibit an exceedingly enhanced activity and selectivity after surface modification with basic and strongly hygroscopic inorganic salts.

Initially, our idea was to modify a commercial Pt/Al₂O₃ catalyst (Alfa Aesar, platinum content 4.86 wt%) with a molten salt coating to benefit from the known low hydrogen solubility of these liquids. In other words, our initial goal was to alter the sorption behavior of substrates and products in methanol steam reforming by the salt coating.^[7]

Chemical modification of heterogeneous catalysts with a thin film of a liquid salt is not new. In literature, this approach has been extensively studied for low melting salts, so-called ionic liquids (ILs), and the term "solid catalyst with ionic liquid layer" (SCILL) has been coined for this approach.^[8] SCILL systems take advantage of specific physicochemical properties of the IL coating (e.g., differential solubility effects),^[7] but also benefit from distinct chemical interactions between the liquid salt and the active surface sites (e.g., alteration of adsorption/desorption processes). The IL film resides on the catalyst surface at conditions of continuous gas phase processes due to its exceedingly low vapor pressure. Remarkable enhancement of selectivity has been observed in a number of hydrogenation reactions after SCILL-type surface modifications (typically at the expense of some activity loss).^[9] Moreover, extensive surface science studies have elucidated the microscopic origin of the observed selectivity effects for SCILL systems.^[10]

From our previous work it was known, that ILs carrying organic heterocyclic cations would not withstand the reaction conditions required for methanol steam reforming.^[11] For the imidazolium cation, it has been found that temperatures above 180 °C in combination with water vapor lead to ring hydrolysis liberating coordinating amines. Therefore, we initially selected the inorganic molten salt mixture Li/K/Cs acetate (molar ratio = 0.2:0.275:0.525)^[12] as coating for the Pt/Al₂O₃ catalyst. Following these first investigations,^[6] the salt selection for catalyst modification has been expanded to alkali hydroxides and carbonates. Note that all successfully applied salts leading to catalyst activation were highly hygroscopic. It was assumed that under reaction conditions a highly concentrated salt solution forms in the catalyst pores regardless of the melting point of the water-free salt. In general, all salt-modified Pt/Al₂O₃ catalysts were obtained by adding a defined amount of salt to the heterogeneous catalyst in form of an aqueous solution, followed by solvent removal and drying under vacuum. The amount of applied salt(s) resulted in a certain mass loading, with *w* being the mass of salt divided by the mass of the uncoated Pt/Al₂O₃ catalyst. All methanol steam reforming experiments were carried out in a continuous fixed bed reactor

setup (see the Supporting Information for details) by bringing the catalyst in contact with a diluted gas stream of methanol and water (in equimolar ratio).

Results and Discussion

Figure 1 shows a comparison of the methanol steam reforming performance of the neat Pt/Al₂O₃ catalyst and the same catalyst coated with a loading of *w* = 30 wt% potassium acetate at *T* = 230 °C under otherwise identical reaction conditions.^[6]

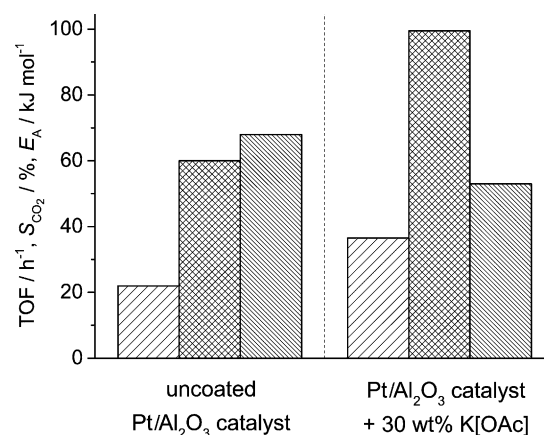


Figure 1. Continuous steam reforming of methanol using the uncoated Pt/Al₂O₃ catalyst (left side) and the Pt/Al₂O₃ catalyst coated with K[OAc] *w* = 30 wt% (right side). TOF (coarse diagonal filling), S_{CO₂} (crossed filling), and E_A (fine diagonal filling); experimental conditions: *T* = 230 °C; *p*_{tot} = 5 bar; *p*_{MeOH} = *p*_{H₂O} = 0.5 bar; *m*_{cat} = 401.4 mg; *τ* = 10 s.

Remarkably, by coating the Pt/Al₂O₃ contact with potassium acetate an increase in activity by a factor of 1.5 and an increase in CO₂ selectivity (S_{CO₂}) from 62% to 99% could be realized. To explain this strong positive effect of the salt coating, a variation in salt loading was carried out. Moreover, coatings with several individual alkali acetates were tested, with the result that potassium acetate shows the strongest enhancement in performance. Anion variation of the salt coating included acetate, hydroxide, hydrogen carbonate and [NTf₂]⁻ salts and revealed that catalyst modification by KOH was the most effective.^[6] We identified three different reasons for the observed enhanced catalytic performance after salt coating: a) alkali doping has been demonstrated to be relevant for the increased CO₂ selectivity; b) the hygroscopic nature of the applied salt was assumed to be relevant for increasing water availability at the catalytic site; and c) the basicity of the salt was regarded to be important for the promotion of the water-gas-shift reaction step, that is, the conversion of CO and water into CO₂ and hydrogen.^[13] The latter reaction forms an important part of the methanol steam reforming reaction sequence.

Based on the particularly promising results for the KOH-coated system, a variation in loading of KOH (3.75, 7.5, 17.15, and 30 wt%) on the Pt/Al₂O₃ contact was performed at a reaction temperature of 230 °C (Figure 2). Although the uncoated reference catalyst showed only a CO₂ selectivity of 62%, the

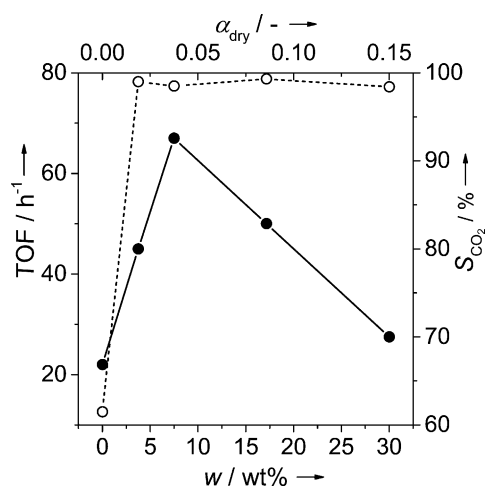


Figure 2. Comparison of TOF (●) and selectivity (○) for a Pt/Al₂O₃ contact coated with four different loadings of KOH (3.75 wt%, 7.5 wt%, 17.15 wt%, 30 wt%) at $T=230^\circ\text{C}$, otherwise equal reaction conditions: $p_{\text{abs}}=5$ bar, $p_{\text{MeOH}}=p_{\text{H}_2\text{O}}=0.5$ bar, $m_{\text{cat.}}=401.4$ mg, $n_{\text{Pt}}=0.10$ mmol, $\tau=10$ s; pore filling degree α_{dry} calculated with $\rho_{\text{KOH}}=2.04$ cm^3g^{-1} .

same contact coated with KOH resulted in selectivities above 99% regardless of the KOH loading. In contrast to this loading-independent step change in selectivity, the observed catalytic activity was quite sensitive to the amount of salt used. The highest activity was obtained for a KOH loading of 7.5 wt% (turnover frequency TOF = 67 h^{-1}), whereas higher salt loadings led to a steep decline in activity. We assume that this is an effect of an increasing share of aqueous salt solution in the pores of the catalyst causing mass transport limitation effects, as will be discussed in detail later. Note that the applied salt loadings caused only low pore filling degrees based on the dry mass of KOH (α_{dry}), but a significant expansion in volume can be expected during water saturation of this salt under reaction conditions.

In a next set of experiments we were interested whether these effects can also be achieved by modification of the catalyst with other alkali hydroxides. LiOH, NaOH, and CsOH were tested; for better comparison the molar amount of salt was kept constant with respect to the sample with 7.5 wt% KOH. This led to applied mass loadings of 3.2 wt% LiOH, 5.35 wt% NaOH, and 20 wt% CsOH. In addition, loadings of 20 wt% LiOH and 20 wt% NaOH as well as 7.5 wt% CsOH were used to test also for potential mass transport limitation effects of these salts. All experiments were carried out at $T=230^\circ\text{C}$ and the results (TOF, S_{CO_2} , activation energy E_A) are presented in Figure 3.

Clearly, all catalysts impregnated with alkali hydroxide salts show better catalytic results than the uncoated reference catalyst. Samples impregnated with KOH or NaOH revealed the highest gain in activity and selectivity. For our reference loading (NaOH: 5.35 wt%; KOH: 7.5 wt%) both, NaOH- and KOH-modified systems result in very similar catalytic activities (TOF_{NaOH}} = 68 h^{-1} ; TOF_{KOH}} = 67 h^{-1}) and a CO₂ selectivity above 99%. Both systems show declining activity with salt amounts above this reference loading. Also the 20 wt% loadings of

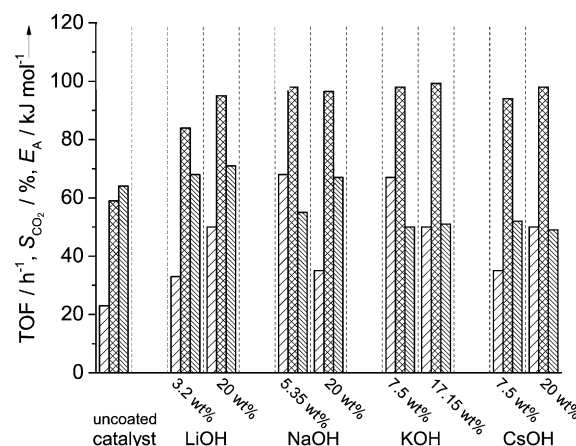


Figure 3. Comparison of catalytic performance of different salt coated Pt/Al₂O₃ catalysts in MeOH steam reforming at $T=230^\circ\text{C}$ variation in salt loading w ; TOF (coarse diagonal filling), S_{CO_2} (crossed filling) and E_A (fine diagonal filling); otherwise identical reaction conditions: $p_{\text{abs}}=5$ bar, $p_{\text{MeOH}}=p_{\text{H}_2\text{O}}=0.5$ bar, $m_{\text{cat.}}=401.4$ mg, $n_{\text{Pt}}=0.10$ mmol, $\tau=10$ s.

LiOH and CsOH coatings led to excellent selectivities but at somewhat lower activity. Considering the activation energies (variation of $T=200\text{--}230^\circ\text{C}$ in steps of 10°C), a difference between the uncoated ($E_A=63$ kJ mol^{-1}) and the hydroxide-coated catalysts (e.g., KOH: $E_A=50$ kJ mol^{-1}) was observed. This could be attributed to a change in reaction mechanism (e.g., different rate-determining step) or an altered adsorption/desorption behavior of reactants (note that changing concentrations/activities of reactants and products with temperature are included in this formal E_A figure).

Diffuse reflectance infrared Fourier transform spectroscopy investigations

It is known that the presence of alkali species in catalyst coatings can result in enhancement of activity and selectivity.^[6] This type of modification, typically referred to as alkali doping, is highly relevant for many industrial catalysts, such as for example, catalysts for ammonia, methanol, and sulfuric acid synthesis, as well as hydrogenation reactions.^[14] For hydrogen production through decomposition of formic acid it has been stated that the reaction rate of a Pd/C catalytic system was enhanced by one to two orders of magnitude through a modification with potassium.^[15] For a ruthenium-based water-gas-shift catalyst it could be shown, that the activity and selectivity was enhanced through an impregnation of the catalytic surface with K₂CO₃.^[16]

To further elucidate the molecular effects of a salt modification on the Pt/Al₂O₃ catalyst in methanol steam reforming we performed diffuse reflectance infrared Fourier transform spectroscopy (DRIFTS). After catalyst preparation (see the Experimental Section) we performed DRIFT spectroscopy to screen the change in CO adsorption at the Pt/Al₂O₃ surface induced by coatings with LiOH, KOH, and CsOH. Again, the molar amount of hydroxide on the catalyst samples was kept equal by applying LiOH, KOH, and CsOH loadings of 3.2 wt%,

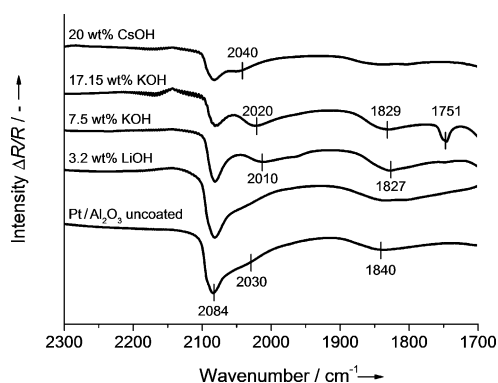


Figure 4. CO region of the DRIFTS spectra for Pt/Al₂O₃ catalysts coated with different alkali hydroxides: LiOH, KOH, and CsOH, compared to the CO adsorption at the uncoated Pt/Al₂O₃ surface.

7.5 wt%, and 20 wt%, respectively. In all cases the molar ratio of alkali metal to platinum (n_{AM}/n_{Pt}) was 5.5. A further experiment with a higher KOH loading ($w = 17.15$ wt%, $n_K/n_{Pt} = 12.3$) was performed to show the influence of higher salt loading. Figure 4 presents the CO region of the corresponding DRIFT spectra for these samples and compares these to the uncoated Pt/Al₂O₃ surface.

In the spectrum for the clean Pt/Al₂O₃ surface, the largest absorption is visible at 2084 cm⁻¹ with a shoulder at 2030 cm⁻¹ and a less intense feature at 1840 cm⁻¹. The catalyst coated with LiOH shows nearly no difference compared to the uncoated sample. Apparently, the amount of LiOH is too low to induce a detectable change in CO adsorption. The spectra for the Pt/Al₂O₃ surface modified with KOH are quite different compared to the unmodified one. The position of the peak at 2084 cm⁻¹ is almost unchanged, but the intensity is nearly halved with the higher loading of KOH ($w = 17.15$ wt%). The shoulder previously located at 2030 cm⁻¹ gains intensity and shifts to lower wavenumbers (2010–2020 cm⁻¹). The peak originally located at 1840 cm⁻¹ also shifts to lower wavenumbers and becomes more intense. For the sample with $w_{KOH} = 17.15$ wt% a new feature appears at 1751 cm⁻¹, which can be attributed to [CO₃]²⁻.^[17] Thus, the band at 1751 cm⁻¹ indicates carbonate formation at least during catalyst preparation.^[17] In the spectrum for 20 wt% CsOH on Pt/Al₂O₃ the decline in intensity at 2084 cm⁻¹ is clearly visible, but the formation of a new band in the range of 1830 cm⁻¹ is only vaguely detectable. We can interpret these spectra based on literature data. The band at 2084 cm⁻¹ is known to correlate with on-top CO adsorbed at terraces, the feature at 2030 cm⁻¹ can be attributed to on-top CO at particle edges, and the initially less intense band at 1840 cm⁻¹ to CO in bridged conformation on terraces.^[18] It is important to note that the measured intensities do not reflect the abundances of adsorbed CO at the different sites because of dipole coupling and intensity transfer arising on metallic surfaces.^[19] Surface science studies for alkali doping provide an interpretation of the observed spectral changes.^[20] The intensity loss of the band at 2084 cm⁻¹ and the shift of the two other bands suggest that the alkali cation displaces CO from the on-top position at terraces and particle edges to

a bridged state on the terraces. Additional effects proposed are short-range interactions between CO and the dopant and an electron transfer from the alkali species to the antibonding 2 π orbitals of CO by means of the platinum d bands.^[20] These effects account for increased CO₂ selectivities during methanol steam reforming. Because of the surface modification with alkali species, adsorbed CO is more tightly bound to the platinum surface and thus the possibility for a consecutive reaction towards CO₂ is enhanced. To further confirm this correlation, we performed CO chemisorption and temperature-programmed desorption (TPD) to analyze the strength of the CO bonding in more detail.

CO Chemisorption–Desorption

All CO chemisorption experiments were carried out by performing CO pulse chemisorption at 40 °C. The catalyst dispersions resulting from surface coating with K[OAc], KOH, and K₂CO₃ were investigated (Figure 5).

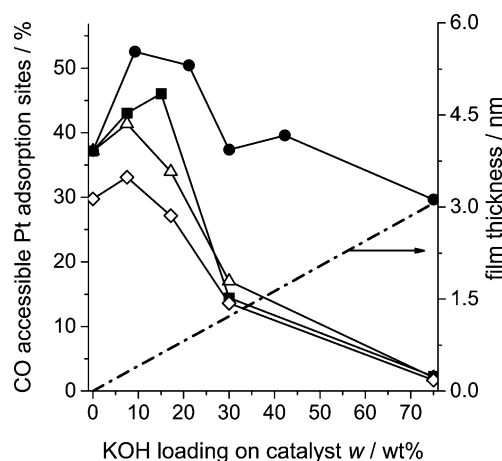


Figure 5. Dispersions measured by CO chemisorption for Pt/Al₂O₃ catalysts coated with different loadings of K[OAc] (■), KOH [ratio 0.8] (◇) and 1 (△), and K₂CO₃ (●).

The dispersion D is determined by the number of platinum adsorption sites measured through CO uptake divided by the total amount of platinum on the catalyst ($D = n_{ads}/n_{Pt}$). Concerning the stoichiometry of CO adsorption at platinum catalysts, stoichiometric factors from 0.7^[21] to 1.0^[22] can be found in the literature. According to the DRIFTS measurements, even for the neat Pt/Al₂O₃ catalyst a small amount of CO is coordinated in bridge-bonded conformation. For the calculation we initially assumed a stoichiometry of 1:1. But for the KOH-coated catalysts, the dispersion was additionally calculated for a stoichiometry of 0.8:1. The mean platinum cluster size can be calculated through the dispersion D . For the uncoated catalyst, the dispersion was estimated to be 37% (1:1 stoichiometry), which implies that 37% of the platinum atoms are located at the cluster surface. From this, a mean platinum cluster diameter of 3 nm can be calculated. Assuming a stoichiometry of 0.8, the dispersion was estimated to be 29.8% resulting in

a mean particle diameter of 3.8 nm (see also TEM image in the Supporting Information, Figure S2). If the catalyst samples were coated with a potassium-containing molten salt, the dispersion values were enhanced for low salt loadings (up to $w = 10$ wt%). Through the modification of the platinum adsorption sites with potassium (alkali doping), the binding sites of CO, the binding energy, and the stoichiometry of CO adsorption are altered.^[17–23] For low salt loadings, potassium-coated Pt/Al₂O₃ catalysts bind more CO than in the unmodified state. This seems to be in conflict with the DRIFTS results on the first view. The shift of CO coordination from the terminal to the bridge-bonded configuration observed in the DRIFTS measurements should result in a lower number of active platinum sites; consequently, the dispersion should be reduced. One possible explanation is the formation of platinum aluminate on the nanoparticle surface resulting in a higher CO accessibility of the remaining Pt⁰ adsorption sites and thus an enhanced platinum dispersion at low salt loadings. However, a strong decline in dispersion was observed for the KOH- and the K[OAc]-coated samples with higher salt loadings. This can be confirmed by the DRIFT spectra. The higher the potassium loading, the more CO is bound in bridge-bonded conformation. A loading of $w = 30$ wt% resulted in a dispersion below 17 wt%. Consequently, less than half of the originally available platinum adsorption sites take part in CO adsorption processes at these high loadings. Additionally, at higher salt loadings ($w = 15$ –75 wt%) occupation of CO adsorption sites by the solid salt takes place under the water-free conditions of this experiment (in contrast to methanol steam reforming). For a loading of $w = 75$ wt% the dispersion was nearly zero ($D = 2\%$), which suggests that the platinum clusters are almost completely covered by the solid and nonporous salt. With a density of KOH in the dry state of 2.04 g cm⁻³ and a catalysts' Brunauer–Emmett–Teller (BET) surface area of 120 m²g⁻¹, the thickness of the salt film (given for KOH in Figure 6) can be calculated for a certain salt loading w . Accordingly, with salt loadings higher than 75 wt% the film becomes thicker than 3 nm and a full coverage of the platinum clusters (mean diameter 3–4 nm) can be

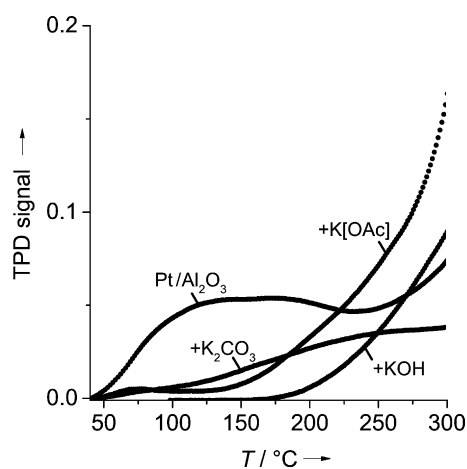


Figure 6. CO-TPD measurements of different catalysts: neat Pt/Al₂O₃, and Pt/Al₂O₃ coated with 30 wt% K[OAc], 21.14 wt% K₂CO₃ and 17.15 wt% KOH (all potassium salts applied in the same molar amount).

expected. Apparently, for catalyst samples coated with K₂CO₃ a different mechanism applies. Here, with low salt loadings, the dispersion was also enhanced compared to the uncoated reference catalyst. But for higher loadings, the drop in dispersion was by far not as pronounced as that of the KOH- and K[OAc]-modified catalysts. With a loading of 75 wt% K₂CO₃ on the catalyst, a dispersion of nearly 30% was retained. Clearly, the K₂CO₃ coating behaves differently in the pores, leaving platinum adsorption sites uncovered and reachable for CO probably due to the porous nature of the solid salt.

In a next set of experiments, we studied CO desorption from the catalyst surface by TPD (Figure 6). For a better comparison, catalysts impregnated with the same molar amount of potassium salt are shown. The neat Pt/Al₂O₃ catalyst shows a first CO desorption maximum at $T = 120$ °C, whereas for the catalysts coated with potassium salts this desorption maximum is shifted towards higher temperatures. The highest shift is found for the KOH-coated catalysts. Note that for the K₂CO₃-impregnated catalyst the CO signal might be overlaid by CO₂ liberated from the carbonate salt [analysis by means of a thermal conductivity detector (TCD)]. The shift in CO desorption temperature is in line with an alkali doping effect caused by all potassium salts. The alkali ion causes a transfer of electron density from the platinum adsorption site to the CO molecule. Consequently, the CO gas is adsorbed more strongly and the desorption temperature, representing bond strength, increases. In other words, the TPD measurements confirm the data from IR spectroscopy, namely that the mode of CO binding is shifted from a terminal/linear to a mainly bridged state (compare section on DRIFTS investigations).^[17–20] The effects of this modified binding mode can be seen in the catalytic results in the methanol reforming reaction. For nearly all alkali-containing Pt/Al₂O₃ catalysts the CO₂ selectivity is significantly increased compared to the unmodified catalyst at a given temperature (compare Figures 3, 7, and 8). This effect is most pronounced for potassium and sodium salt coatings. Despite the shift in desorption temperature, CO desorption is observed above $T = 200$ °C for the KOH-impregnated sample. Thus, it is reasonable that CO₂ selectivity is lower than 100% above 200 °C under conditions of methanol steam reforming. Another interesting question

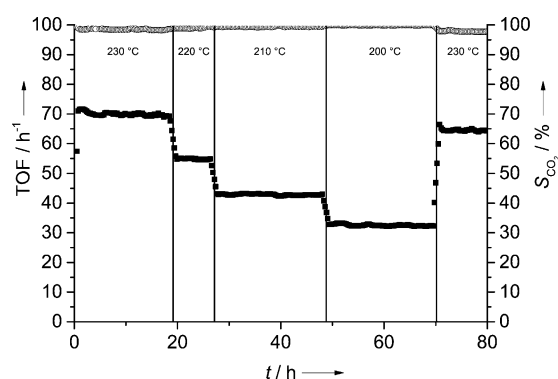


Figure 7. Continuous steam reforming of methanol using the KOH-coated Pt/Al₂O₃ catalyst, $w = 7.5$ wt% (■: TOF; ○: selectivity). Experimental conditions: $T = 230$ – 200 °C (see vertical lines); $p_{\text{tot}} = 5$ bar; $p_{\text{MeOH}} = p_{\text{H}_2\text{O}} = 0.5$ bar; $m_{\text{cat}} = 401.4$ mg; $\tau = 10$ s.

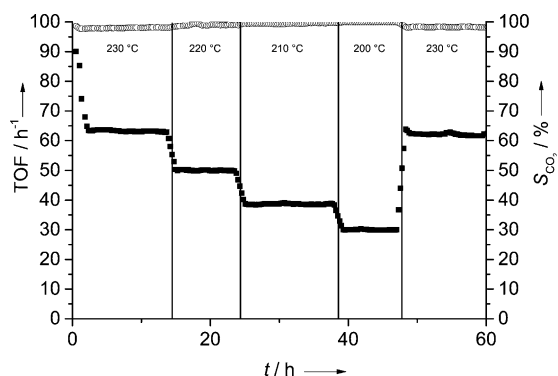


Figure 8. Continuous steam reforming of methanol using the K_2CO_3 -coated $\text{Pt}/\text{Al}_2\text{O}_3$ catalyst, $w = 9.2$ wt% (■: TOF; ○: selectivity). Experimental conditions: $T = 230$ – 200 °C (see vertical lines); $p_{\text{tot}} = 5$ bar; $p_{\text{MeOH}} = p_{\text{H}_2\text{O}} = 0.5$ bar; $m_{\text{cat}} = 401.4$ mg; $\tau = 10$ s.

pertains to the interaction of the salt coating with the reaction product CO_2 . This influence was probed by comparing methanol steam reforming for $\text{Pt}/\text{Al}_2\text{O}_3$ catalysts impregnated with KOH and K_2CO_3 , respectively.

Comparison of KOH- and K_2CO_3 -impregnated catalysts

Clearly, KOH coatings on the $\text{Pt}/\text{Al}_2\text{O}_3$ catalyst convert to the corresponding carbonate in the presence of the reaction product CO_2 . Therefore, we were interested in studying a catalyst sample coated directly with K_2CO_3 . The loading was chosen to provide an identical potassium-to-platinum ratio. Thus, the amount of impregnated carbonate salts corresponds to the expected loading after full transformation of a 7.5 wt% KOH loading with CO_2 . Figures 7 and 8 compare these two KOH- and K_2CO_3 -coated catalysts in methanol steam reforming under otherwise identical reaction conditions.

Indeed, the KOH and the K_2CO_3 coating of $\text{Pt}/\text{Al}_2\text{O}_3$ catalysts results in nearly identical performance in methanol steam reforming. At $T = 230$ °C, the KOH-coated sample reaches a TOF of 70 h^{-1} in the beginning and deactivates to 63 h^{-1} after 80 h reaction time, whereas the K_2CO_3 -impregnated catalyst shows an activity of 63 h^{-1} . Both catalysts possess a CO_2 selectivity larger than 98% at $T = 230$ °C. Initially, the K_2CO_3 sample reveals a much higher apparent activity. This value must be corrected, however, by the fact that additional CO_2 is liberated from the K_2CO_3 coating at the beginning of the catalytic test in the process of establishing an equilibrium between carbonate, water, hydroxide, and CO_2 under reaction conditions. Extra CO_2 formed by carbonate decomposition exits the reactor during the first 2 h time on stream (TOS) and is quantified together with the CO_2 from methanol steam reforming (measured by gas chromatography), thus influencing the measured activity. An opposite situation is found in the case of the KOH coating. Here, CO_2 from the steam reforming reaction is taken up by the KOH coating to form carbonate species on the catalyst surface. This CO_2 uptake by the catalyst results in an apparently lower catalytic activity as it leads to a reduced amount of detectable CO_2 at the reactor outlet. Apart from these well-understandable differences in the first couple of hours on stream,

both the KOH- and the K_2CO_3 -coated catalysts show stable and remarkably similar performance (TOF is in a range of $\pm 2 \text{ h}^{-1}$).

Phase behavior of KOH– H_2O saturated with K_2CO_3

As all reaction processes in methanol steam reforming occur necessarily in the presence of water vapor, we considered in our following experiments the phase behavior of the system KOH– H_2O – K_2CO_3 to gain more insight into the processes at the catalysts' surfaces. Figure 9 shows the literature-known phase diagram of the system KOH– H_2O under the assumption of saturation with K_2CO_3 .^[24,25]

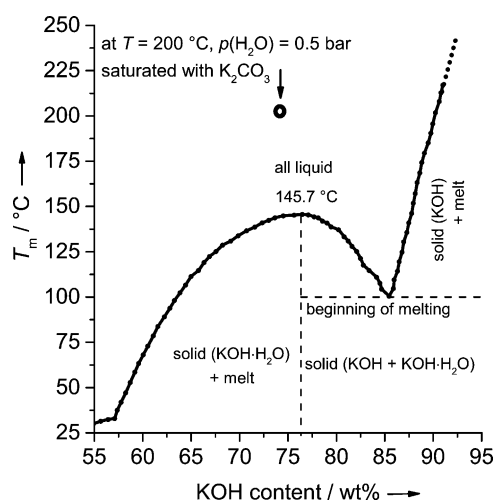


Figure 9. Phase behavior of the system KOH– H_2O saturated with K_2CO_3 ($\text{K}_2\text{CO}_3/\text{KOH}$ weight ratio = 0.032) adapted after Refs. [24, 25].

Apparently, under reaction conditions of methanol steam reforming ($T = 200$ °C; $p_{\text{H}_2\text{O}} = 0.5$ bar), a liquid film composed of 73.5 wt% KOH (saturated with K_2CO_3) and 26.5 wt% H_2O is formed on the catalysts surface. To obtain the phase diagram shown in Figure 9, the original diagram^[25] was modified using the freezing temperatures measured by Vogel et al. for a K_2CO_3 -saturated KOH– H_2O mixture in the range of 70–85 wt% KOH ($\text{K}_2\text{CO}_3/\text{KOH}$ weight ratio = 0.032).^[24] The composition was determined from the vapor pressure curves over molten KOH– H_2O – K_2CO_3 at $T = 200$ °C and $p_{\text{H}_2\text{O}} = 0.5$ bar. With this composition one can estimate the melting point of the respective KOH– H_2O mixture to 143.5 °C. Consequently, under reaction conditions, a highly concentrated, aqueous salt solution is present on the active sites of the catalyst surface. Additionally, the pore-filling degree α , as given for dry KOH in Figure 2, has to be corrected under the real conditions of catalysis ($T = 200$ °C, $p_{\text{H}_2\text{O}} = 0.5$ bar, 73.5 wt% KOH, 26.5 wt% H_2O). Under these conditions, the density of the salt solution is $\rho = 1.68 \text{ g cm}^{-3}$ in comparison to $\rho = 2.04 \text{ g cm}^{-3}$ for KOH in the dry state.^[24] Thus, the pore-filling degrees under real catalytic conditions have to be corrected by a factor of roughly 1.2. This has been realized in Figure 10, which displays TOF/selectivity vs. real loading of the salt solution.

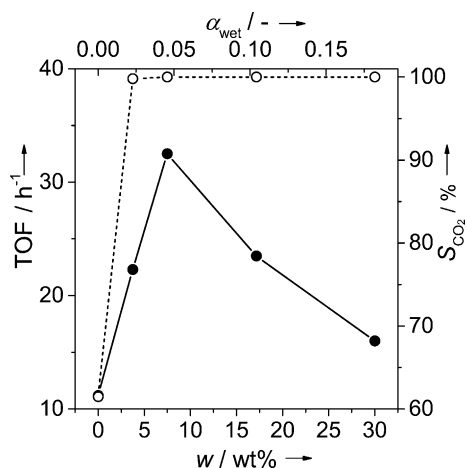


Figure 10. Comparison of TOF (●) and selectivity (○) for catalysts loaded with four different amounts of KOH (3.75 wt%, 7.5 wt%, 17.15 wt%, 30 wt%) at $T=200\text{ }^{\circ}\text{C}$, the data on the x -axis represents the resulting loading with aqueous salt solution under the applied reaction conditions: $p_{\text{abs}}=5\text{ bar}$, $p_{\text{MeOH}}=p_{\text{H}_2\text{O}}=0.5\text{ bar}$, $m_{\text{cat.}}=401.4\text{ mg}$, $n_{\text{Pt}}=0.10\text{ mmol}$, $\tau=10\text{ s}$; pore filling degree α_{wet} calculated with $\rho_{\text{KOH}}=1.68\text{ cm}^3\text{ g}^{-1}$.

The general trends in Figure 10 are similar to those in Figure 2 with the best system still remaining the one with a dry loading of 7.5 wt% KOH. Again, a clear reduction in catalyst activity is observed for the higher pore-filling degrees. This raises the question whether at high pore-filling degrees the overall reaction rate may be influenced by fluid–fluid mass transport effects.

Dynamic vapor sorption experiments with alkali hydroxide-coated catalysts

As a first step towards addressing this question we probed the adsorption equilibrium of water with the KOH-coated Pt/Al₂O₃ catalysts by dynamic vapor sorption (DVS) experiments. For this purpose, the catalyst samples were dried prior to testing ($T=300\text{ }^{\circ}\text{C}$, $t=240\text{ min}$). Then, the samples were contacted with gas streams of different humidity at $T=40\text{ }^{\circ}\text{C}$ and the resulting mass changes were recorded. All values in Figure 11 were recorded after the samples reached equilibrium at each humidity step, that is, until their change in mass was less than 0.001 \% min^{-1} .

The DVS experiments reveal that the uncoated Pt/Al₂O₃ catalyst shows an almost linear water uptake up to a 12 wt% water content at a relative humidity $\phi=80\%$. After coating the Pt/Al₂O₃ with KOH water adsorption significantly increases. Catalyst coating with $w=7.5\text{ wt\% KOH}$ results in a water uptake of nearly 30 wt% at 80% humidity. With 17.15 wt% salt coating the water uptake is as high as 50 wt% at 80% humidity. From the shape of the adsorption isotherms for the KOH-coated samples one can conclude that linear surface adsorption of water takes place at low humidity $\phi<40\%$. We interpret the increasing relative water uptake at a humidity $\phi>40\%$ as an additional absorption of water in the formed hydroxide/water layer on the catalyst surface.

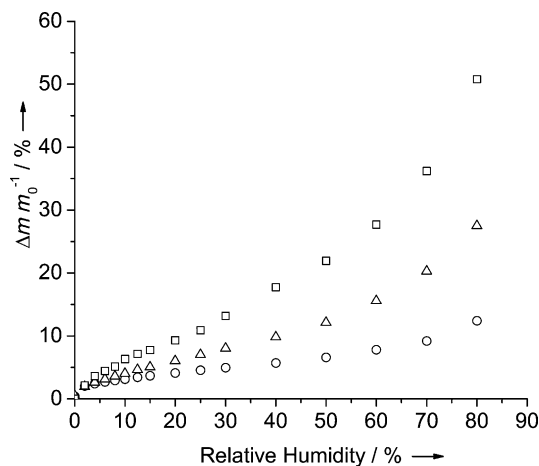


Figure 11. Dynamic vapor sorption for the Pt/Al₂O₃ catalysts (○) and the catalysts coated with $w=7.5\text{ wt\% KOH}$ (△) or $w=17.15\text{ wt\% KOH}$ (□) at $T=40\text{ }^{\circ}\text{C}$, relative humidity ϕ was varied from 0 to 80%.

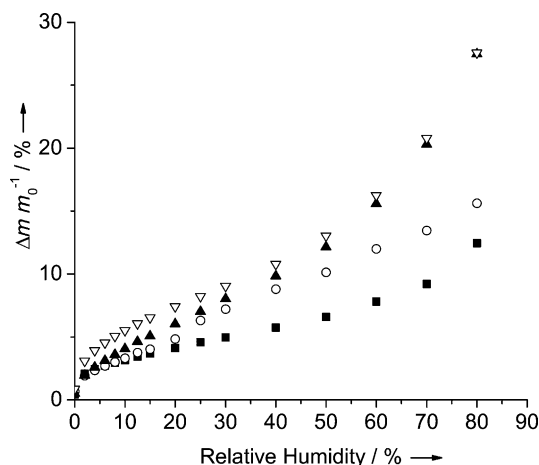


Figure 12. Dynamic vapor sorption for the Pt/Al₂O₃ catalysts (■) and the catalysts coated with $w=3.2\text{ wt\% LiOH}$ (○), $w=7.5\text{ wt\% KOH}$ (▲) and $w=20\text{ wt\% CsOH}$ (▼) at $T=40\text{ }^{\circ}\text{C}$, relative humidity ϕ varied from 0 to 80%.

In the next set of experiments we compared the water sorption behavior of several alkali hydroxides coated onto the Pt/Al₂O₃ catalyst. All catalysts were prepared with the same molar amount of hydroxide, resulting in mass loadings of $w=3.2\text{ wt\% LiOH}$, 7.5 wt\% KOH , and 20 wt\% CsOH , respectively (see Figure 12). The adsorption isotherm for the LiOH-coated catalyst sample results in a straight line with a maximum water uptake of 15 wt% at $\phi=80\%$. Keeping in mind that the water solubility for LiOH is relatively low ($127.4\text{ g L}^{-1}\text{ LiOH}$; $1278\text{ g L}^{-1}\text{ KOH}$; $3000\text{ g L}^{-1}\text{ CsOH}$ at $T=30\text{ }^{\circ}\text{C}$)^[26] and that the corresponding lithium aluminate is not soluble in water, one can assume that for the LiOH-coated catalysts predominantly surface adsorption is taking place. The trend of the adsorption isotherms for the KOH- and CsOH-coated samples is nearly identical. Both samples take up water up to roughly 15% at a humidity of 60% and roughly 28 wt% at a humidity of 80% and show the same nonlinear behavior of their isotherms. Our previous assumption that the nonlinear behavior of the isotherms at high

humidity is due to water absorption into a salt/water liquid film is further confirmed by the fact that cesium aluminate shows deliquescence in the presence of moisture (see also the ^{27}Al magic-angle spinning (MAS) NMR measurements probing aluminate formation).^[27] In conclusion from our DVS experiments it is highly likely that water condensation within the catalyst pores takes place to a significant extent and is further promoted by the type and amount of salt coating. This results in a relatively high degree of liquid filling in the pore system and increases the probability of mass transfer limitations at the fluid–fluid transition.

Probing the influence of mass transfer on the overall observed reaction rate

For these investigations we focused on the $\text{Pt}/\text{Al}_2\text{O}_3$ catalyst loaded with $w = 17.15$ wt% KOH. This loading shows already a decline in activity compared to lower salt loadings (compare Figure 2 and Figure 10). Moreover, this sample shows the highest water uptake in the DVS experiments, producing a high degree of pore filling with a liquid in the catalyst during reaction. Note that the $\text{KOH}-\text{H}_2\text{O}$ system should be liquid under reaction conditions of methanol steam reforming (as shown in Figure 9).

To test for diffusion influences, two experimental runs with different catalyst masses were performed under otherwise equal reaction conditions. The methanol inlet stream was varied and the methanol conversion X was plotted against the modified residence time $m_{\text{cat}} \cdot n_{\text{MeOH},0}^{-1}$ (Figure 13). In such an

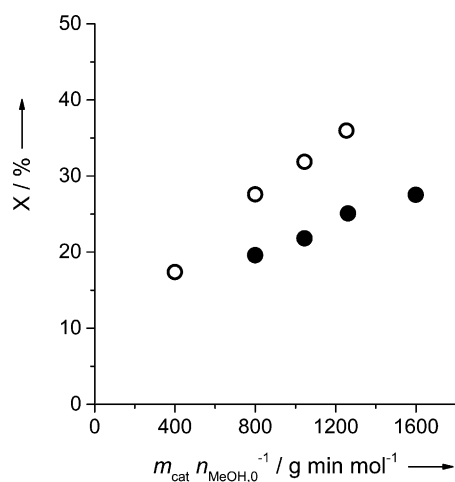


Figure 13. Test for film diffusion influence in methanol steam reforming at $T = 230^\circ\text{C}$: catalyst loaded with $w = 17.15$ wt% KOH, $m_{\text{cat,uncoated}} = 200.7$ mg (\circ), $m_{\text{cat,uncoated}} = 401.4$ mg (\bullet); otherwise the same reaction conditions: $p_{\text{abs}} = 5$ bar, $p_{\text{MeOH}} = p_{\text{H}_2\text{O}} = 0.5$ bar, $\tau = 10\text{--}40$ s.

experiment the reaction would be identified as being kinetically controlled if the two graphs for the two catalyst loadings are identical.^[28] However, Figure 13 shows that the two conversion vs. modified residence time graphs do not concur for the two different amounts of catalyst. Therefore, we can conclude that for the case of a $\text{Pt}/\text{Al}_2\text{O}_3$ catalyst loaded with $w =$

17.15 wt% KOH mass transfer effects influence the observed overall reaction rate.

^{27}Al solid state NMR measurements

To shed more light on the role of salt coating on the nature of the alumina support, ^{27}Al solid-state MAS NMR measurements have been carried out, both before the reaction (hydroxide-coated $\text{Pt}/\text{Al}_2\text{O}_3$ catalysts heated to 150°C for 4 h without contact with reactants) and after the reaction ($T = 200\text{--}230^\circ\text{C}$, $p_{\text{H}_2\text{O}} = p_{\text{MeOH}} = 0.5$ bar, $t = 80$ h on stream). Figure 14 shows the

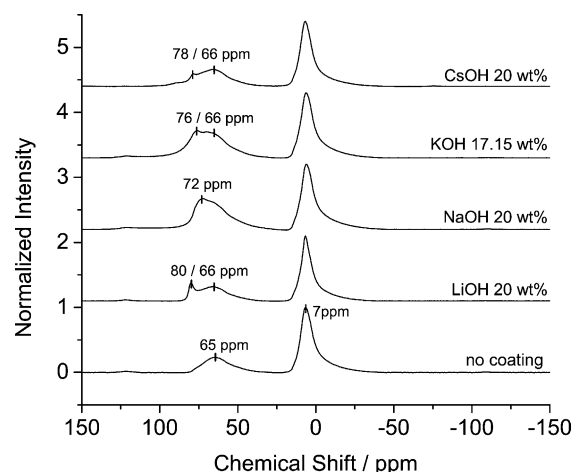


Figure 14. ^{27}Al solid-state MAS NMR measurements of $\text{Pt}/\text{Al}_2\text{O}_3$ coated with alkali hydroxides before methanol steam reforming reaction (samples heated to 150°C , $t = 4$ h).

^{27}Al MAS NMR spectra for the alkali hydroxide-coated $\text{Pt}/\gamma\text{-Al}_2\text{O}_3$ catalyst. For the uncoated reference $\text{Pt}/\gamma\text{-Al}_2\text{O}_3$ catalyst two broad resonances are identified. One with a maximum at 7 ppm assigned to octahedrally coordinated aluminum atom in the alumina, whereas the other peak maximum at 65 ppm can be assigned to tetrahedrally coordinated aluminum atoms. Although the spectra acquired are not quantitative, they were used for comparison purposes within this study, keeping in mind that the aluminum site ratios may not represent all aluminum sites present. The ratio of tetrahedral to octahedral aluminum is 30:70 as known from the literature.^[29] For the $\text{Pt}/\text{Al}_2\text{O}_3$ catalysts impregnated with LiOH and heated to 150°C (before reaction, without contact to the reactants water and methanol), the tetrahedral resonance splits into two, with a new narrow peak maximum appearing at 80 ppm, which can be attributed to a lithium aluminate species.^[30] Additionally, the ratio of tetrahedrally to octahedrally coordinated aluminum atoms is shifted to 35:65. This shift is reasonable due to the tetrahedral nature of the aluminum in the alkali aluminate. For the other alkali hydroxide coatings, similar effects are observed. For the NaOH-coated $\text{Pt}/\text{Al}_2\text{O}_3$, the new peak maximum occurs at 72 ppm (tetr./oct. = 50:50), for the KOH-modified $\text{Pt}/\text{Al}_2\text{O}_3$, a new peak arises at 76 ppm (tetr./oct. = 50:50), and for the CsOH-impregnated sample, a new peak (tetr./oct. = 32:68) can be identified at 78 ppm. We interpret these findings in the

following way: By modifying the Pt/Al₂O₃ catalysts with alkali hydroxides the alumina surface reacts to form surface aluminate, that is, a more basic surface layer on the alumina support. Under the applied conditions support transformation to the aluminate is far from complete as indicated by the ²⁷Al MAS NMR spectra. Note that in the case of LiOH coating a loading of *w* = 100 wt% would be necessary for a complete transformation to the lithium aluminate. Unfortunately, it is not possible to judge from these experiments whether the formed aluminate exists in a partially hydrated form, as hydrated aluminates exhibit nearly identical chemical shifts compared to the non-hydrated ones.^[27]

During methanol steam reforming, the as-prepared hydroxide-coated catalysts are in contact with water and methanol. After the reaction, the catalyst samples were analyzed using ²⁷Al MAS NMR. The results are summarized in Figure 15. These NMR spectra indicate that except for the LiOH-coated catalyst

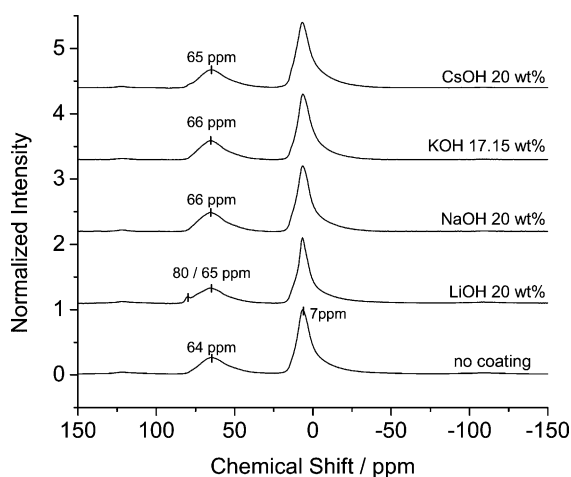


Figure 15. ²⁷Al solid-state MAS NMR measurements of Pt/Al₂O₃ coated with alkali hydroxides after continuous methanol steam reforming reaction (varied *T* = 200–230 °C, *p*_{H₂O} = 0.5 bar, *t*_{mean, reaction} = 80 h).

all indications for alkali aluminate peaks have disappeared. For the uncoated Pt/Al₂O₃ reference catalyst no obvious change is detectable between the catalyst before reaction and after operation. Again, two peak maxima are visible at 7 and 64 ppm, reflecting tetrahedrally and octahedrally coordinated aluminum atoms with a ratio of 30 to 70. Interestingly and in contrast to the situation before methanol steam reforming, the NaOH-, KOH-, and CsOH-coated catalysts show no aluminate peak in the MAS NMR spectra after methanol steam reforming. In addition, the ratio of tetrahedrally to octahedrally coordinated aluminum atoms has returned for all three catalysts to a 30:70 ratio. Only the NMR data for the LiOH-modified catalyst still show a small aluminate signal maximum at 80 ppm with the ratio tetrahedral to octahedral being 33:67. We take these results as strong indication that the sodium, potassium, or cesium aluminate formed at the alumina surface during catalyst preparation is hydrolyzed during methanol reforming, resulting in alumina coated with the corresponding hydroxide, hydrates thereof, or alkaline aqueous solution (in accordance

to earlier literature on the hydrolysis of aluminates^[31]). In the presence of methanol, the solubility of alumina should be further reduced^[32] so that partial alumina precipitation can be expected when methanol is present during the steam reforming reaction. We conclude from these findings that during methanol steam reforming the salt coating acts not only in the form of a chemical support modification but also as a fluid-side induced modification of the catalytic platinum sites.

To verify our hypothesis of in situ aluminate formation in the preparation of alkali hydroxide-coated catalysts, we prepared mixtures of alumina and the corresponding alkali hydroxides in stoichiometric ratios to induce complete aluminate formation. These samples were heated to 400 °C for 12 h and immediately analyzed using MAS NMR spectroscopy to avoid contact with moisture. The resulting data are shown in the Supporting Information. Except for LiOH/alumina full conversion towards the alkali aluminate species is reached under these conditions. In the case of the LiOH-containing sample, full conversion to the aluminate is most likely prevented by the relatively low solubility of LiOH in water (preparation as dispersion: alumina powder in LiOH/water). All peak maximum positions of the thus prepared aluminates are nearly equal to the ones found for the alkali hydroxide-coated Pt/Al₂O₃ catalyst prior to steam reforming reaction (see Figure 14).

Conclusions

We have demonstrated a synthetically straightforward procedure to drastically enhance the performance of heterogeneous Pt/Al₂O₃ catalysts in methanol steam reforming. The procedure is simple, robust, and economically attractive and thus of potential technical relevance. Our spectroscopic findings indicate that alkali doping, especially with potassium, plays an important role in activation of platinum. In addition, hygroscopicity and basicity of the applied molten salt contribute to the significant increase in catalytic activity and selectivity. We found evidence that under reaction conditions an (at least partly) liquid film of alkali hydroxide/alkali carbonate is formed on the catalyst/alumina surface. This hydroxide/water film increases the availability of water at the active catalyst sites. However, with too much salt present, the resulting high liquid pore filling introduces mass transfer impediments as evidenced by our kinetic studies. Thus, the best compromise between beneficial catalyst modification and introduction of additional mass transfer barriers is obtained at relatively low amounts of salt coatings, typically at 5–10 wt% salt loading. Although in the dry preparation of alkali hydroxide salts on Pt/Al₂O₃ evidence for surface aluminate formation is found, this support modification is not expected to play a major role during catalysis as in the presence of water and methanol the aluminate hydrolyses and no indication for surface aluminate is found after the reaction, at least with the most active KOH coating.

We anticipate that the modification of heterogeneous catalysts by molten salts can be transferred to other industrially relevant reactions in the future. Moreover, this SCILL approach using molten salts opens a new way to a rational and cost-effi-

cient approach to optimize heterogeneous catalysts through surface modification or co-adsorption effects.

Experimental Section

Materials

Platinum on aluminum oxide was purchased from Alfa Aesar (LOT: F02R004, precise platinum content = 4.86 wt%). Lithium acetate, potassium acetate, cesium acetate, potassium hydrogen carbonate, and potassium carbonate were obtained from Sigma Aldrich with a purity of 99.99% and dried prior to use/weighing (120 °C, vacuum, at least 2 h). Lithium hydroxide (Merck, >98%), sodium hydroxide (Merck, >99%), potassium hydroxide (Merck, >85%, rest H₂O, K₂CO₃ <1%), and cesium hydroxide (Fluka, 95%, rest H₂O) were used as stock solution, the amount of hydroxide was determined by titration with 1 M HCl (Merck).

Synthesis of salt-modified catalysts

The calculated amount of platinum on support was immersed into a solution of the salt or salt mixture in high-purity water (typically 20 mL). After mixing for 30 min at 25 °C the solvent was removed by means of a vacuum (55 °C, 80 mbar). The alkali hydroxide-coated catalysts/samples were heated to 150 °C under vacuum (<0.1 mbar) for at least 4 h prior to the methanol steam reforming experiments. The same procedure was applied prior to the CO chemisorption and MAS NMR experiments.

Catalytic experiments

The catalyst performance in methanol steam reforming was evaluated in a continuously operated gas-phase fixed-bed reactor similar to the one described elsewhere^[33] (details are found in the Supporting Information). An equimolar mixture of methanol and water was evaporated and fed to the reactor. At the reactor outlet, unconverted methanol and water were condensed and the product gas was analyzed by GC (Varian CP 4900). Catalyst activities are provided as TOF, which is the total molar flow of carbon monoxide, carbon dioxide, and methane divided by the total molar amount of platinum in the reactor (typically 0.1 mmol). S_{CO_2} is given as the CO₂ mol fraction in the outlet gas stream divided by the sum of CO₂, CO, and CH₄. The mass balance was closed by the quantification of the inert gas nitrogen.

DRIFTS experiments

The catalyst characterization was performed in a Bruker Vertex 80v infrared spectrometer equipped with a Praying Mantis and a High Temperature Reaction Chamber (HVC-DRP-4) from Harrick. An extension with all necessary feedthroughs was adjoined to the sample chamber of the spectrometer to allow the evacuation of the optical path. Mass flows and pressures were adjusted using Bronkhorst mass flow and pressure controllers. Prior to CO adsorption, the catalyst powder was heated under argon flow (Linde, >99.9999%, 10 mL_N min⁻¹, 1 bar) at 300 °C for 30 min to desorb water and other contaminations. After exposure to CO (Linde, >99.997%, 10 mL_N min⁻¹) at 35 °C for 10 min, the reactor was purged thoroughly with Ar for 60 min until no CO gas phase signal could be detected anymore. The IR spectra were recorded with a spectral resolution of 2 cm⁻¹, 1024 scans, and a scan speed of

40 kHz. The reference spectrum was pristine alumina exposed to the same treatment.

CO chemisorption experiments

CO chemisorption experiments were carried out under dynamic conditions in a Micromeritics Autochem 2920. The catalyst samples were heated to 300 °C (10 K min⁻¹, 30 min isothermal, helium atmosphere) prior to CO adsorption. CO was dosed to the sample ($T=40$ °C) through a loop ($V=500$ μL), and the sagged CO was detected by means of a TCD. For the calculation of dispersion D a adsorption stoichiometry of 1:1 was supposed for all catalyst samples (if not otherwise indicated). CO desorption was performed by heating the sample to 500 °C (10 K min⁻¹, 60 min isothermal, helium atmosphere), detection by means of a TCD.

Diffusion limitation testing

The applied testing method for film diffusional influences is based on literature methods.^[28] Two methanol reforming experiments were performed using two different masses of catalyst (1st run: $m_{\text{cat., uncoated}}=200.7$ mg; 2nd run: $m_{\text{cat., uncoated}}=401.4$ mg). The methanol inlet stream was adapted to the catalysts masses to realize comparable modified residence times $m_{\text{cat.}}/n_{\text{MeOH, in}}$. All other experimental conditions were kept identical: $T=230$ °C; catalyst loaded with 17.15 wt% KOH; $p_{\text{abs}}=5$ bar; $p_{\text{MeOH}}=p_{\text{H}_2\text{O}}=0.5$ bar; $\tau=10$ –40 s. The evaluation was based on methanol conversion.

Dynamic vapor sorption experiments

The water adsorption isotherms of the alkali hydroxide-coated catalysts were recorded by performing dynamic vapor sorption in a DVS elevated temperature system (DVS-ET) from Surface Measurement Systems. All measurements were performed in nitrogen ($V=200$ mL min⁻¹). The adsorption isotherms were recorded at $T=40$ °C with ultrapure water. Prior to adsorption the samples were heated to $T=300$ °C (25 to 100 °C, 32.5 min; 100 °C isothermal for 60 min; 100 to 300 °C, 100 min; 300 °C isothermal for 240 min; 300 to 25 °C, 90 min). Typically, a mass of 8–10 mg of catalyst was used.

Solid-state ²⁷Al MAS NMR experiments

All 1D single-pulse ²⁷Al solid-state MAS NMR spectra were recorded at room temperature on an Agilent DD2 500WB spectrometer at a resonance frequency of 130.24 MHz, using a sample spinning rate of 15 kHz. The powder samples were packed into 3.2 mm zirconia rotors equipped with a Torlon spacer and caps. 2000 scans were accumulated for qualitative spectra using a 2 μs 90° pulse and a 1 s recycle delay. The chemical shifts were referenced according to IUPAC guidelines.

Acknowledgements

The authors acknowledge financial support by the Deutsche Forschungsgemeinschaft (DFG) within the Excellence Cluster "Engineering of Advanced Materials" in the framework of the excellence initiative. M.K., F.A., N.N.B., and P.W. would like to thank the EU for support through its ERC Advanced Investigator Grant No. 267376. Furthermore, A.K., M.L., and J.L. acknowledge addi-

tional support by the Fonds der Chemischen Industrie, DAAD, and the COST Action CM1104.

Keywords: catalyst characterization · heterogeneous catalysis · methanol reforming · molten salts · platinum

- [1] J. Agrell, B. Lindström, L. J. Pettersson, S. G. Järas, *Catalysis* **2002**, *16*, 67–132.
- [2] G. A. Olah, A. Goepfert, G. K. S. Prakash, *Beyond Oil and Gas. The Methanol Economy*, Wiley-VCH, Weinheim, **2009**.
- [3] C. Wannek in *Hydrogen Energy* (Ed.: D. Stolten), Wiley-VCH, Weinheim, **2010**, pp. 17–40.
- [4] D. R. Palo, R. A. Dagle, J. D. Holladay, *Chem. Rev.* **2007**, *107*, 3992–4021.
- [5] S. Sá, H. Silva, L. Brandão, J. M. Sousa, A. Mendes, *Appl. Catal. B* **2010**, *99*, 43–47.
- [6] M. Kusche, F. Enzenberger, S. Bajus, H. Niedermeyer, A. Bösmann, A. Kaftan, M. Laurin, J. Libuda, P. Wasserscheid, *Angew. Chem. Int. Ed.* **2013**, *52*, 5028–5032; *Angew. Chem.* **2013**, *125*, 5132–5136.
- [7] V. A. Cocalia, A. E. Visser, R. D. Rogers, J. D. Holbrey in *Ionic Liquids in Synthesis* (Eds.: P. Wasserscheid, T. Welton), Wiley-VCH, Weinheim, **2008**, pp. 89–102.
- [8] U. Kernchen, B. Etzold, W. Korth, A. Jess, *Chem. Eng. Technol.* **2007**, *30*, 985–994.
- [9] a) J. Arras, M. Steffan, Y. Shayeghi, D. Ruppert, P. Claus, *Green Chem.* **2009**, *11*, 716–723; b) J. Arras, E. Paki, C. Roth, J. Radnik, M. Lucas, P. Claus, *J. Phys. Chem. C* **2010**, *114*, 10520–10526.
- [10] a) M. Sobota, M. Happel, M. Amende, N. Paape, P. Wasserscheid, M. Laurin, J. Libuda, *Adv. Mater.* **2011**, *23*, 2617–2621; b) H.-P. Steinrück, J. Libuda, P. Wasserscheid, T. Cremer, C. Kolbeck, M. Laurin, F. Maier, M. Sobota, P. S. Schulz, M. Stark, *Adv. Mater.* **2011**, *23*, 2571–2587.
- [11] N. Taccardi, D. Assenbaum, M. E. M. Berger, A. Bösmann, F. Enzenberger, R. Wölfel, S. Neuendorf, V. Göke, N. Schrödel, H.-J. Maass, H. Kistenmacher, P. Wasserscheid, *Green Chem.* **2010**, *12*, 1150–1156.
- [12] G. G. Diogenov, G. S. Sergeeva, *Zh. Neorg. Khim.* **1965**, *10*, 292–294.
- [13] a) M. Haukka, T. Venäläinen, M. Kallinen, T. A. Pakkanen, *J. Mol. Catal. A* **1998**, *136*, 127–134; b) Y. Zhai, D. Pierre, R. Si, W. Deng, P. Ferrin, A. U. Nilekar, G. Peng, J. A. Herron, D. C. Bell, H. Saltsburg, M. Mavrikakis, M. Flytzani-Stephanopoulos, *Science* **2010**, *329*, 1633–1636.
- [14] W. D. Mross, *Catal. Rev. Sci. Eng.* **1983**, *25*, 591–637.
- [15] D. A. Bulushev, L. Jia, S. Beloshapkin, J. R. H. Ross, *Chem. Commun.* **2012**, *48*, 4184–4186.
- [16] B. Liu, T. Huang, Z. Zhang, Z. Wang, Y. Zhang, J. Li, *Catal. Sci. Technol.* **2014**, *4*, 1286–1292.
- [17] B. W. Krupay, Y. Amenomiya, *J. Catal.* **1981**, *67*, 362–370.
- [18] a) N. R. Avery, *Appl. Surf. Sci.* **1982**, *13*, 171–179; b) B. E. Heyden, A. M. Bradshaw, *Surf. Sci.* **1983**, *125*, 787–802; c) C. W. Olsen, R. I. Masel, *Surf. Sci.* **1988**, *201*, 444–460.
- [19] a) P. Hollins, *Surf. Sci. Rep.* **1992**, *16*, 51–94; b) F. M. Hoffmann, *Surf. Sci. Rep.* **1983**, *3*, 107–192.
- [20] H. P. Bonzel, *Surf. Sci. Rep.* **1988**, *8*, 43–125.
- [21] R. K. Herz, D. F. McCready, *J. Catal.* **1983**, *81*, 358–368.
- [22] a) V. Perrichon, L. Retailleau, P. Bazin, M. Daturi, J. C. Lavaelly, *Appl. Catal. A* **2004**, *260*, 1–8; b) A. Renouprez, C. Hoang-Van, P. A. Compagnon, *J. Catal.* **1974**, *34*, 411–422; c) H. Matsuhashi, S. Nishiyama, H. Miura, K. Eguchi, K. Hasegawa, Y. Iizuka, A. Igarashi, N. Katada, J. Kobayashi, T. Kubota, T. Mori, K. Nakai, N. Okazaki, M. Sugioka, T. Umeki, Y. Yazawa, D. Lu, *Appl. Catal. A* **2004**, *272*, 329–338.
- [23] K. Foger, J. R. Anderson, *Appl. Surf. Sci.* **1979**, *2*, 335–351.
- [24] W. M. Vogel, K. J. Routsis, V. J. Kehrer, D. A. Landsman, J. G. Tschinkel, *J. Chem. Eng. Data* **1967**, *12*, 465–471.
- [25] E. Lang, *Hooker Chemical Co.*, **1949**.
- [26] D. R. Lide in *Handbook of Chemistry and Physics, Internet Version 2005*, CRC Press, Boca Raton, FL, **2005**, 1351–1359.
- [27] R. Hoppe, H.-P. Müller, *Solid State Ionics* **1990**, *43*, 23–30.
- [28] J. Hagen in *Chemische Reaktionstechnik* (Ed.: V. Hopp), Wiley-VCH, Weinheim, **1992**, pp. 83–89.
- [29] M.-H. Lee, C.-F. Cheng, V. Heine, J. Klinowski, *Chem. Phys. Lett.* **1997**, *265*, 673–676.
- [30] a) D. Müller, W. Gessner, A. Samoson, E. Lippma, G. Scheler, *J. Chem. Soc. Dalton Trans.* **1986**, *6*, 1277–1281; b) D. Müller, W. Gessner, H.-J. Behrens, G. Scheler, *Chem. Phys. Lett.* **1981**, *79*, 59–62.
- [31] a) Y. Zhang, Y. Li, Y. Zhang, *J. Chem. Eng. Data* **2003**, *48*, 617–620; b) S. Ma, S. Zheng, Y. Zhang, *J. Chem. Eng. Data* **2007**, *52*, 77–79.
- [32] Y. Zhang, S. Zheng, H. Du, S. Wang, Y. Zhang, *J. Chem. Eng. Data* **2010**, *55*, 1237–1240.
- [33] S. Werner, N. Szesni, A. Bittermann, M. J. Schneider, P. Härter, M. Hausmann, P. Wasserscheid, *Appl. Catal. A* **2010**, *377*, 70–75.

Received: April 28, 2014

Revised: June 12, 2014

Published online on August 14, 2014